A Novel CD135$^+$ Subset of Mouse Monocytes with a Distinct Differentiation Pathway and Antigen-Presenting Properties

Naoka Kamio,*,†,‡,[1] Asumi Yokota,‡,§,[1] Yuichi Tokuda,¶ Chie Ogasawara,‖ Masakazu Nakano,¶ Miki Nagao,* Kei Tashiro,¶ Taira Maekawa,†,# Nobuyuki Onai,‖ and Hideyo Hirai*,†,‡

The mononuclear phagocyte system (MPS), composed of monocytes/macrophages and dendritic cells (DCs), plays a critical role at the interface of the innate and adaptive immune systems. However, the simplicity of MPS has been challenged recently by discoveries of novel cellular components. In the current study, we identified the CD135$^+$ subset of monocytes as a novel class of APCs in mice. CD135$^+$ monocytes were readily found in the bone marrow, spleen, and peripheral blood at steady state, and they expressed markers specific to DCs, including MHC class II and CD209a, along with markers for monocytes/macrophages. In addition, this subset phagocytosed bacteria and activated naive T lymphocytes, fulfilling the criteria for APCs. CD135$^+$ monocytes were derived directly from macrophage DC progenitors, not from common monocyte progenitors or other monocytes, suggesting that these are distinct from conventional monocytes. These findings facilitate our understanding of the MPS network that regulates immune responses for host defense. ***The Journal of Immunology*****, 2022, 209: 498–509.**

Dendritic cells (DCs) play a central role in the immune system by connecting innate and adaptive immunity. Conventional DCs (cDCs) sense and ingest external Ags and present them on MHC class II, which activates naive T lymphocytes (1–4). In addition to cDCs, monocyte-derived DCs (moDCs) and plasmacytoid DCs (pDCs) are present in both mice and humans (5–7). All of these DC types are crucial for immune responses and maintenance of homeostasis. moDCs are induced in response to microbial infections and regulate the function of CD4$^+$ or CD8$^+$ T lymphocytes by presenting ingested Ags (7–9). pDCs, originating from both myeloid and lymphoid progenitors (10), secrete type I IFN upon their activation by signals mediated through TLR7 and TLR9 during viral infections (11, 12).

DCs and monocytes/macrophages compose the mononuclear phagocyte system (MPS), and they are generally considered to originate from common progenitor cells in the bone marrow (BM), although arguments still remain (1, 13–15). Macrophage DC progenitors (MDPs) are considered to reside at the top of the hierarchy within the MPS, giving rise to both monocyte and DC lineages (16). Common DC progenitors (CDPs) (17) and common monocyte progenitors (cMoPs) (18) have been identified as exclusive progenitors for DCs and monocytes, respectively. MDPs and CDPs, both of which are progenitors of cDCs and pDCs, express Flt3 (also known as CD135) on their surface. *Flt3* mRNA was detected in short-term hematopoietic stem cells, and the expression peaked in multipotent progenitors (19). Progenitor cells retaining surface CD135 expression have the potential to give rise to DCs, whereas progenitors, which no longer express CD135, lose their ability to differentiate into DCs. Also, the number of DCs is significantly reduced in the absence of Flt3 signaling, suggesting a critical role for the Flt3 ligand (Flt3L)–Flt3 interaction in the development of DC lineages (2, 20, 21).

moDCs are distinct from other DCs as they are generally considered to originate from monocytes rather than from undifferentiated progenitors (6, 22). Under inflammatory conditions, monocytes acquire CD11c and MHC class II expression, which indicates their differentiation into moDCs (23–26). In addition, large numbers of moDCs can be obtained by in vitro culture of monocytes (7, 27, 28). Therefore, moDCs have been widely used for intensive characterization of DCs and have been used in immunotherapies (29, 30).

Accumulating evidence has shown that monocytes are a heterogeneous population in mice and humans (14, 31, 32). In mice, monocytes are classified based on the expression level of Ly6C. Ly6C^{high} and Ly6C^{low} monocytes represent "classical" and "nonclassical" monocytes, respectively (33, 34). In addition, recent technical advances, including single-cell analysis, have further extended our understanding

*Department of Clinical Laboratory Medicine, Kyoto University Hospital, Kyoto, Japan; †Department of Transfusion Medicine and Cell Therapy, Kyoto University Hospital, Kyoto, Japan; ‡Laboratory of Stem Cell Regulation, School of Life Sciences, Tokyo University of Pharmacy and Life Sciences, Tokyo, Japan; §Divisions of Pathology and Experimental Hematology and Cancer Biology, Cincinnati Children's Hospital Medical Center, OH; ¶Department of Genomic Medical Sciences, Kyoto Prefectural University of Medicine, Kyoto, Japan; ‖Department of Immunology, Kanazawa Medical University, Japan; and #Kyoto Prefectural Institute of Public Health and Environment, Kyoto, Japan

[1]N.K. and A.Y. contributed equally to this work.

ORCIDs: 0000-0001-6720-2158 (M. Nakano), 0000-0002-8886-6145 (M. Nagao).

Received for publication January 12, 2021. Accepted for publication May 24, 2022.

This work was partly supported by KAKENHI Grants-in-Aid for Scientific Research from the Japan Society for the Promotion of Science and University Grants 18K08354, 21K19386 and 21H02956 (to H.H.) and 21K08379 (to A.Y.).

N.K.: methodology, validation, formal analysis, investigation, writing – original draft and visualization; C.O.: investigation; Y.T., M. Nakano, and K.T.: validation, formal analysis, and writing – review and editing; A.Y.: validation and formal analysis, investigation, and writing – review and editing; M. Nagao and T.M.: supervision; N.O.: methodology, validation, formal analysis, and writing – review and editing; H.H.: conceptualization, methodology, validation, formal analysis, writing – review and editing, project administration, and funding acquisition.

The sequences presented in this article have been submitted to the DNA Data Bank of Japan under accession numbers E-GEAD-338 and DRA009516.

Address correspondence and reprint requests to Dr. Hideyo Hirai, Laboratory of Stem Cell Regulation, School of Life Sciences, Tokyo University of Pharmacy and Life Sciences, 1432-1 Horinouchi, Hachioji, Tokyo 192-0392, Japan. E-mail address: hirai@toyaku.ac.jp

The online version of this article contains supplemental material.

Abbreviations used in this article: BM, bone marrow; cDC, conventional DC; cDC2, cDC type 2; CDP, common DC progenitor; cMoP, common monocyte progenitor; DC, dendritic cell; DC-SIGN, DC-specific ICAM-3–grabbing nonintegrin; DTR, diphtheria toxin receptor; Flt3L, Flt3 ligand; FPKM, fragments per kilobase of transcript per million mapped reads; iNOS, inducible NO synthase; Lin, lineage; MDP, macrophage DC progenitor; moDC, monocyte-derived DC; MPS, mononuclear phagocyte system; NGS, next-generation sequencing; PB, peripheral blood; pDC, plasmacytoid DC; RNA-seq, RNA sequencing.

of MPS diversity (35–37). Hence, elucidation of the cellular components within the MPS is necessary for the precise understanding of the immune system and for their clinical application. During our attempts to characterize monocyte subpopulations, we have identified a unique $CD135^+$ population among cells expressing CD115 and CD11b, the markers that conventionally define monocytes. We propose that this population, based on its functions and differentiation pathway, represents a novel class of APCs.

Materials and Methods

Mice

C57BL/6 mice ($CD45.2^+$, 7–12 wk old) were purchased from CLEA Japan (Tokyo, Japan) or Tokyo Laboratory Animals Science (Tokyo, Japan). BALB/c mice (7–12 wk old) were purchased from Japan SLC (Shizuoka, Japan). $CD45.1^+$ in C57BL/6 background mice were a gift from Shigekazu Nagata (Osaka University, Osaka, Japan). All of the animal protocols were approved by the Committee on Animal Research of the Kyoto University Faculty of Medicine and by the Tokyo University of Pharmacy and Life Sciences Animal Use Committee.

Csf2$^{-/-}$ (38), *Csf2rb*$^{-/-}$ (39), *Flt3l*$^{-/-}$ (40), CD11c–diphtheria toxin receptor (DTR) (41), and CX_3CR1-GFP mice (42) were maintained in the specific pathogen-free facility at Kanazawa Medical University, and all experiments with these animals were also approved by the Institutional Animal Care Committees of Kanazawa Medical University.

Flow cytometric analysis and cell sorting

To obtain BM cells, tibia, femur, and humerus were flushed with PBS containing 2% FCS. Peripheral blood (PB) samples were collected from the orbital venous plexus under anesthesia. To lyse RBCs, BM, spleen, or PB cells were treated with Pharm Lyse reagent (BD Biosciences, San Jose, CA). For surface marker staining, cells were stained with the fluorescent marker-conjugated Abs listed in Supplemental Table I. Propidium iodide was used to exclude dead cells.

To analyze the effect of LPS, 5 μg of LPS (*Escherichia coli* O111:B4, Sigma-Aldrich, St. Louis, MO) was injected i.p. 12 h prior to analysis.

The CD11c-DTR mice were injected i.p. with 4 ng/g body weight DT (Sigma-Aldrich) in PBS. BM cells were analyzed by flow cytometry 1, 2, 3, 4, and 5 d after the DT injection.

BM cells were collected from wild-type, *Csf2*$^{-/-}$, *Csf2rb*$^{-/-}$, and *Flt3l*$^{-/-}$ mice and analyzed by flow cytometry.

A BD Cytofix/Cytoperm plus fixation/permeabilization kit with GolgiStop (BD Biosciences) was used for intracellular staining of cytokines. To investigate the effect of LPS on the production of inducible NO synthase (iNOS) or TNF-α, purified cells were incubated in cell culture medium in the presence of 1 μg/ml LPS for 16 h. Flow cytometric analyses or sorting were performed using FACSCanto II or FACSAria III (BD Biosciences). Data were analyzed using FlowJo software (BD Biosciences).

RNA sequencing

Total RNA was extracted using a RNeasy micro kit (Qiagen, Valencia, CA). Quantity and quality of RNA samples from each mouse were confirmed using an Agilent 2200 TapeStation (Agilent Technologies). The cDNA libraries for next-generation sequencing (NGS) were constructed using a Smart-Seq v4 ultra low input RNA kit for sequencing (Clontech), a Nextera XT DNA library preparation kit (Illumina), and a Nextera XT index kit (Illumina), according to the manufacturers' instructions. The quality of NGS libraries was assessed using a fragment analyzer (Agilent) and sequenced on a NovaSeq 6000 System (Illumina) using a NovaSeq Xp 4-Lane Kit. Base calls were converted to the fastq file format by bcl2fastq2 conversion software v2.20 (Illumina). Library preparation and sequencing were performed at Takara Bio (Shiga, Japan), and the fastq files were provided to the NGS Core Facility of Kyoto Prefectural University of Medicine for further analyses.

RNA sequencing data analyses

RNA sequencing (RNA-seq) reads from the fastq files were aligned to Ensembl GRCm38/mm10 genome assembly by using Tophat 2.0.9 with Bowtie2 version 2.1.0 and samtools 0.1.19 after performing the quality control with FASTX-Toolkit 0.0.13, FastQC version 0.11.2, and PRINSEQ lite version 0.20.4. Gene expression analysis was performed on FPKM (fragments per kilobase of transcript per million mapped reads) data calculated from the RNA-seq data using Cufflinks 2.2.1. For the cell clustering, principal component and heatmap analyses were carried out using R version 3.6.0. Finally, 4891 genes were selected for analyses based on the results from the Cuffdiff option of Cufflinks under the following quality control conditions: 1) excluding genes where the "status" was not "OK," 2) excluding genes that showed an error value for "log2(fold_change)," 3) including genes that showed "yes" for "significant," 4) including genes that resulted in a $|\log_2(\text{fold change})| \geq 2.0$, and 5) excluding genes when more than six samples resulted in FPKM = 0. For the heatmap analysis of myeloid transcription factor genes, the heatmap images were drawn using the pheatmap package after normalizing the FPKM values derived from 27 selected genes by using the zFPKM R/Bioconductor package. The images of RNA-seq data were drawn using the Integrative Genomics Viewer tool (43).

Giemsa staining

Cytospin specimens were stained using a Diff-Quik stain kit (Sysmex, Kobe, Japan), a modified Wright–Giemsa staining system (44). To analyze the dendrite formation by $CD135^+$ monocytes, cells were incubated for 16 h in RPMI 1640 cell culture medium supplemented with 10 ng/ml GM-CSF (FUJIFILM Wako Pure Chemical Corporation, Osaka, Japan), 10% FCS, 50 μM 2-ME, and penicillin-streptomycin. Images were captured using an Olympus BX43 microscope (Olympus, Tokyo, Japan) connected to a DP80 CCD camera, and processed using cellSens standard 1.12 software (Olympus).

Phagocytosis assay

Sorted cells were cultured in RPMI 1640 cell culture medium supplemented with 10% FCS, 50 μM 2-ME, and penicillin-streptomycin with or without 5 ng/ml LPS for 2 h. Then, pHrodo Red *E. coli* BioParticles conjugate for phagocytosis (Invitrogen, Carlsbad, CA), whose fluorescence was activated only when ingested and acidified by phagocytes, was added to the culture and incubated in a 37°C water bath or on ice for 1 h. The cells were directly analyzed by flow cytometry.

MLR assay

$CD4^+$ T cells were isolated from the spleen of BALB/c (H-2^d) or C57BL/6 (H-2^b) mice for allogeneic and autologous reactions, respectively, using an EasySep mouse T cell isolation kit (STEMCELL Technologies, Vancouver, BC, Canada) in combination with biotin-conjugated CD8 Abs to remove $CD8^+$ T cells. Purified $CD135^-$ monocytes, $CD135^+$ monocytes, cDCs, and pDCs obtained from the BM of C57BL/6 mice were used as test cells. To investigate the effect of LPS, these sorted cells were incubated in cell culture medium containing 5 ng/ml LPS for 2 h and washed twice and then subjected to MLR. Test cells (1×10^4) were incubated with 5×10^4 autologous or allogeneic $CD4^+$ T cells, which had been stained using a CellTrace Violet cell proliferation kit (Invitrogen, Carlsbad, CA) in wells of a 96-well U-bottom culture plate. After 4 d of coculture, proliferation of the T cells was assessed by flow cytometry.

Adoptive transfer experiment

Sorted cells from $CD45.1^+$ or $CD45.2^+$ mice were resuspended in 30 μl of PBS and injected directly into the tibial BM cavity of $CD45.2^+$ or $CD45.1^+$ mice, respectively (45). After 48 (for monocytes), 60 (for progenitors), or 108 h (for $CD135^+$ monocytes and progenitors), BM from the injected tibia and spleen cells of the recipients were collected and subjected to flow cytometric analysis.

Statistical analysis

Statistical analyses were performed using Microsoft Excel. Statistical differences were determined using a Student *t* test or the Tukey test. Values of $p < 0.05$ were considered statistically significant.

Data and materials availability

Sequence data were deposited to the DNA Data Bank of Japan. Accession numbers for the Genomic Expression Archive and the DNA Data Bank of Japan Sequence Read Archive are E-GEAD-338 (https://ddbj.nig.ac.jp/public/ddbj_database/gea/experiment/E-GEAD-000/E-GEAD-338/) and DRA009516 (https://ddbj.nig.ac.jp/resource/sra-submission/DRA009516), respectively.

Results

Identification of $CD135^+$ monocytes

Mouse monocytes are identified as $CD11b^+CD115^+$ cells within lineage marker (CD3, CD19, NK1.1, Ter119, and Ly6G)–negative (Lin^-) BM or PB cells, and they are composed of at least two subpopulations, $Ly6C^{high}$ classical and $Ly6C^{low}$ nonclassical or "patrolling" monocytes (34, 46). During our attempts to identify monocyte subpopulations, we

found that a small proportion of monocytes expressed CD135 in the BM (right lower panel in Fig. 1A). Whereas CD135$^-$ monocytes were clearly divided into Ly6C^{high} and Ly6C^{low} subsets, the expression level of Ly6C on CD135$^+$ monocytes was continuously distributed from intermediate to high (i.e., Ly6C^{int} to Ly6C^{high}). These CD135$^+$ monocytes were consistently found in spleen and PB as shown in Fig. 1B. Giemsa staining revealed that Ly6C^{high}CD135$^-$ monocytes were mononuclear cells with bean-shaped nuclei and that Ly6C^{low}CD135$^-$ monocytes were homogeneously smaller cells with horseshoe-shaped or bilobular nuclei (Fig. 1C). Both Ly6C^{high} and Ly6C^{int} CD135$^+$ monocytes were morphologically similar to the Ly6C^{high}CD135$^-$ monocytes. In this study, we focused on the Ly6C^{high} and Ly6C^{int} CD135$^+$ monocyte subsets.

CD135$^+$ monocytes express markers of DCs

CD135 is the receptor of Flt3L, an indispensable cytokine for differentiation and maintenance of DCs (2, 21). To assess the significance of CD135 on CD135$^+$ monocytes, we analyzed *Flt3l*$^{-/-}$ mice (38–40) and found that both Ly6C^{high} and Ly6C^{int} CD135$^+$ monocytes in the BM of these mice were significantly decreased when compared with those in wild-type mice (Fig. 2A). *Flt3l* deficiency also caused significant reduction of MDPs and CDPs, in addition to CD135$^+$ monocytes (Fig. 2D, 2F), whereas the number of Ly6C^{high}, Ly6C^{low} CD135$^-$ monocytes or cMoPs was not affected (Fig. 2B, 2C, and 2E, respectively). The numbers of CD135$^+$ monocytes and those of MDPs and CDPs were unchanged in the BM of *Csf2*$^{-/-}$ mice and *Csf2rb*$^{-/-}$ mice (38–40), suggesting the dependence of CD135$^+$ monocyte differentiation on Flt3L but not on GM-CSF.

Next, we analyzed the expression of DC markers on CD135$^+$ monocytes (Fig. 3, Supplemental Fig. 1, under the PBS-treated condition). CD11c and MHC class II were highly expressed by cDCs (CD3$^-$, CD19$^-$, NK1.1$^-$, CD11c^{high} B220$^-$ cells in the spleen) and expressed at a low level by CD135$^-$ monocytes (Supplemental Fig. 1). CD135$^+$ monocytes expressed CD11c and MHC class II at an intermediate level (Fig. 3A). Accordingly, both Ly6C^{high} and Ly6C^{int} CD135$^+$ monocytes in the BM of CD11c-DTR mice, which express DTR under the control of a CD11c promoter (41), were transiently and significantly reduced by DT administration (Fig. 3B, left panel), whereas CD135$^-$ monocytes were not affected (Fig. 3B, right panel).

CD209a (DC-specific ICAM-3–grabbing nonintegrin [DC-SIGN]), a C-type lectin receptor known to be specific to DCs (35), was highly expressed on CD135$^+$ monocytes but at a marginal level on CD135$^-$ monocytes, and the pDC marker Siglec-H (47) was expressed on Ly6C^{high} and Ly6C^{int} CD135$^+$ monocytes at a low level comparable to that on CD135$^-$ monocytes (Fig. 3A, Supplemental Fig. 1A).

As previous reports have shown that infection and inflammation promote differentiation and maturation of moDCs (48), we investigated the effects of LPS administration on DC marker expression on CD135$^+$ monocytes. When wild-type mice were administered LPS i.p., the numbers of Lin$^-$ CD115-expressing cells, including MDPs, cMoPs, CDPs, and all subsets of monocytes, were significantly decreased (data not shown). In response to LPS, expression of CD11c and MHC class II on CD135$^+$ monocytes was markedly upregulated (Fig. 3A). The costimulation molecules CD40, CD80, and CD86 were expressed at low levels by CD135$^+$ monocytes in the steady state, but highly upregulated in response to in vivo LPS stimulation (Fig. 3A). When Ly6C^{high} and Ly6C^{int} CD135$^+$ monocytes were cultured in the presence of GM-CSF for 16 h, dendrites were induced, indicating differentiation toward DC-like cells (Fig. 3C).

In addition, we analyzed the expression of other myeloid cells markers. The macrophage marker F4/80 was expressed on both Ly6C^{high} and Ly6C^{int} CD135$^+$ monocytes at a level comparable to that found on Ly6C^{high} and Ly6C^{low} CD135$^-$ monocytes (Fig. 3A, Supplemental Fig. 1A). CD16/32, SIRPα, PD-L1, and PD-L2 were also expressed on CD135$^+$ monocytes at levels comparable to those on CD135$^-$ monocytes (Supplemental Fig. 2A). CD64, FcεRI, CCR2, and CX_3CR1 are expressed on monocytes and/or moDCs (7, 14). We observed that expression levels of these molecules on

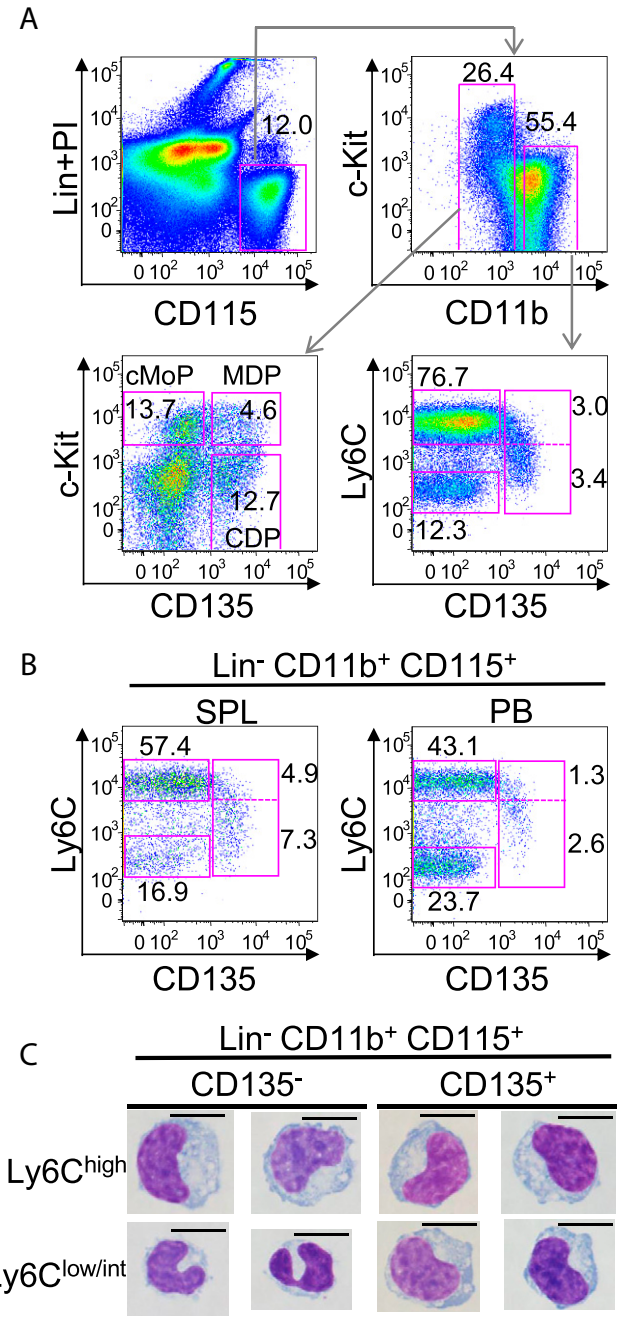

FIGURE 1. Identification of CD135$^+$ subsets of monocytes. (**A**) Flow cytometric analysis of mouse bone marrow (BM) cells. Lineage (Lin)$^-$ markers and propidium iodide (PI)$^-$ CD115$^+$ cells (left upper panel) were divided into CD11b$^-$ and CD11b$^+$ subpopulations (right upper panel). CD11b$^-$ and CD11b$^+$ subpopulations were further subdivided based on c-Kit/CD135 or Ly6C/CD135 expression, respectively (lower panels). CDP, common dendritic cell progenitor; cMoP, common monocyte progenitor; MDP, macrophage dendritic cell progenitor. (**B**) Flow cytometric analysis of mouse Lin$^-$CD11b$^+$CD115$^+$ spleen (SPL) and peripheral blood (PB) monocytes. CD135$^+$ cells were detected in the Lin$^-$CD11b$^+$CD115$^+$ monocyte fraction of BM, spleen, and PB cells (A and B). (**C**) Giemsa staining of subpopulations of Lin$^-$CD11b$^+$CD115$^+$ monocytes. Scale bars, 10 μm.

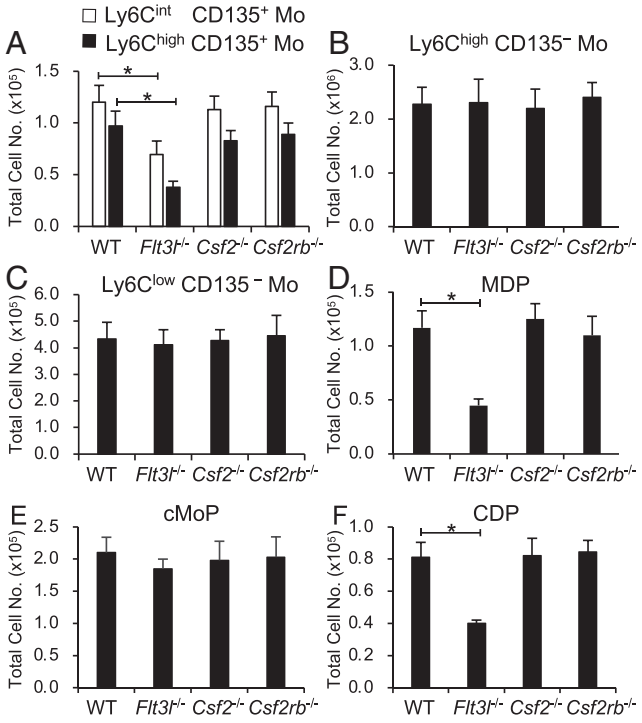

FIGURE 2. Differentiation of Ly6C^{high} and Ly6C^{int} CD135$^+$ monocytes is dependent on Flt3. (**A**–**F**) The total numbers of Ly6C^{high} and Ly6C^{int} CD135$^+$ monocytes (A), Ly6C^{high} and Ly6C^{low} CD135$^-$ monocytes (B and C, respectively), macrophage dendritic cell progenitors (MDPs) (D), common monocyte progenitors (cMoP) (E), and common dendritic cell progenitors (CDPs) (F) in the bone marrow of wild-type (WT), *Flt3l*$^{-/-}$, *Csf2*$^{-/-}$, and *Csf2rb*$^{-/-}$ mice are shown. Data are means ± SD of three mice (*$p < 0.05$, determined by Student *t* test).

CD135$^+$ monocytes were similar (CD64, FcεRI, and CCR2) or slightly higher (CX_3CR1) than those on Ly6C^{high} CD135$^-$ monocytes (Supplemental Fig. 2B, 2C). When compared with cDCs type 2 (cDC2s), lower FcεRI and higher CCR2 expression were distinct phenotypes of CD135$^+$ monocytes. cDC2s expressed CX_3CR1 in a biphasic manner, but shared expression of other myeloid markers with CD135$^+$ monocytes (Supplemental Fig. 2A, 2B). Collectively, both Ly6C^{high} and Ly6C^{int} CD135$^+$ monocytes harbored characteristics of DCs in addition to monocytic features, and these DC-like phenotypes were enhanced in response to LPS or GM-CSF.

CD135$^+$ monocytes are a distinct subset of monocytes

Since we observed that CD135$^+$ monocytes, composing a small minority of Lin$^-$CD11b$^+$CD115$^+$ monocytes, possessed not only the characteristics of monocytes but also of DCs, we hypothesized that CD135$^-$ monocytes are the conventional monocytes and CD135$^+$ monocytes represent a novel distinct subset. Therefore, we analyzed the comprehensive gene expression profiles of these populations by RNA-seq to define their hierarchical and relative position in the MPS (Fig. 4). To this end, we purified Ly6C^{high} and Ly6C^{int} subsets of CD135$^+$ monocytes from BM and compared their transcriptional profiles with those of conventional Ly6C^{high} and Ly6C^{low} monocytes, MDPs, cMoPs, and CDPs obtained from BM and cDC2s (CD11b$^+$CD8$^-$ cDCs) obtained from the spleen. cDC2s were chosen because of their similarity to CD135$^+$ monocytes in terms of CD11b expression (49). First, unsupervised clustering of the gene expression showed very similar gene expression profiles for Ly6C^{high} and Ly6C^{int} CD135$^+$ monocytes (Fig. 4A). The first branching in the hierarchical clustering dendrogram was a division into two groups, the progenitor cluster (MDPs, cMoPs, and CDPs) and the differentiated cell cluster (Ly6C^{high} and Ly6C^{low} CD135$^-$ monocytes, Ly6C^{high} and Ly6C^{int} CD135$^+$ monocytes, and cDC2s). Within the differentiated cell cluster, CD135$^+$ monocytes were closer to CD135$^-$ monocytes than to cDC2s (Fig. 4A). Accordingly, principal component analysis showed that gene expression profiles of these populations were divided into the progenitor group and the differentiated cell group (Fig. 4B). Profiles of the Ly6C^{high} and Ly6C^{int} CD135$^+$ monocytes were distinct from other differentiated cells and resided between Ly6C^{high} and Ly6C^{low} CD135$^-$ monocytes and cDC2s, which indicates that CD135$^+$ monocytes possess characteristics intermediate between CD135$^-$ monocytes and cDC2s. Among the myeloid transcription factors analyzed (Fig. 4C), *Klf4* was expressed by both CD135$^-$ and CD135$^+$ monocytes at relatively high levels, while higher expression of *Batf3*, *Irf4*, and *SpiB* were shared by Ly6C^{high} and Ly6C^{int} CD135$^+$ monocytes and cDC2s. *Irf8*, *Tcf4*, and *Slfn5* were highly expressed by CD135$^+$ monocytes at the level similar to progenitors (*Irf8* and *Tcf4*) or to Ly6C^{high}CD135$^-$ monocytes (*Slfn5*) (Fig. 4C). *SpiC and Hes1* were highly expressed by CD135$^-$ monocytes and cDC2s, whereas CD135$^+$ monocytes and progenitors expressed these genes at a lower level (Fig. 4C). The pattern of genes expressed by CD135$^+$ monocytes suggests that they are a distinct subpopulation of monocytes that harbors characteristics intermediate between conventional monocytes and cDCs.

CD135$^+$ monocytes express genes related to phagocytosis and Ag presentation

Having confirmed that CD135$^+$ monocytes represent a distinct population, we looked for genes highly expressed by these cells (Fig. 5). First, we focused on classical and nonclassical MHC class II genes, which are required for Ag presentation to CD4$^+$ T cells (Fig. 5A, 5B). Ly6C^{int}CD135$^+$ monocytes expressed classical MHC class II genes, including *H2-Aa*, *H2-Ab1*, and *H2-Eb1*, at levels comparable to those of cDC2s, whereas Ly6C^{high}CD135$^+$ monocytes were similar to Ly6C^{low}CD135$^-$ monocytes. Among the cells examined, nonclassical MHC class II genes such as *H2-Oa*, *H2-Ob*, and *H2-DMb2* were expressed at the highest levels by cDC2s. The expression level of these genes in Ly6C^{int}CD135$^+$ monocytes was lower than in cDC2s, but higher than in Ly6C^{high}CD135$^+$ monocytes or conventional CD135$^-$ monocytes, which is consistent with the intermediate characteristics of CD135$^+$ monocytes shown in Fig. 4. Next, we focused on DC-SIGN genes (Fig. 5C). Among the cells examined, *Cd209a*, *Cd209b*, *Cd209c*, *Cd209d*, and *Cd209e* were expressed at the highest levels by Ly6C^{high} and Ly6C^{int} CD135$^+$ monocytes. Other genes encoding Fc receptors, complement receptors, TLRs, and integrins were expressed by CD135$^+$ monocytes at levels similar to those by Ly6C^{high}CD135$^-$ monocytes (data not shown).

Then, we sought for CD135$^+$ monocytes specific markers and found that *Cd301a* (*Clec-10a*) and *Cd206* (*Mrc1*) genes were highly expressed by Ly6C^{high} and Ly6C^{int} CD135$^+$ monocytes (Supplemental Fig. 3). CD301a is a C-type lectin, and CD206, also a C-type lectin, is a mannose receptor. We evaluated the expression of these molecules at the protein level by flow cytometry and confirmed their high expression in Ly6C^{high} and Ly6C^{int} CD135$^+$ monocytes (Supplemental Fig. 3). However, CD301a was also expressed by Ly6C^{high}CD135$^-$ monocytes and the expression of CD206 on CD135$^+$ monocytes was not high enough, suggesting the need for more ideal specific markers. Taken together, the unique expression of MHC class II genes, DC-SIGNs, and other molecules related to recognition of microorganisms, phagocytosis, and Ag presentation by the CD135$^+$ monocyte subpopulation suggests its functional properties within the immune system.

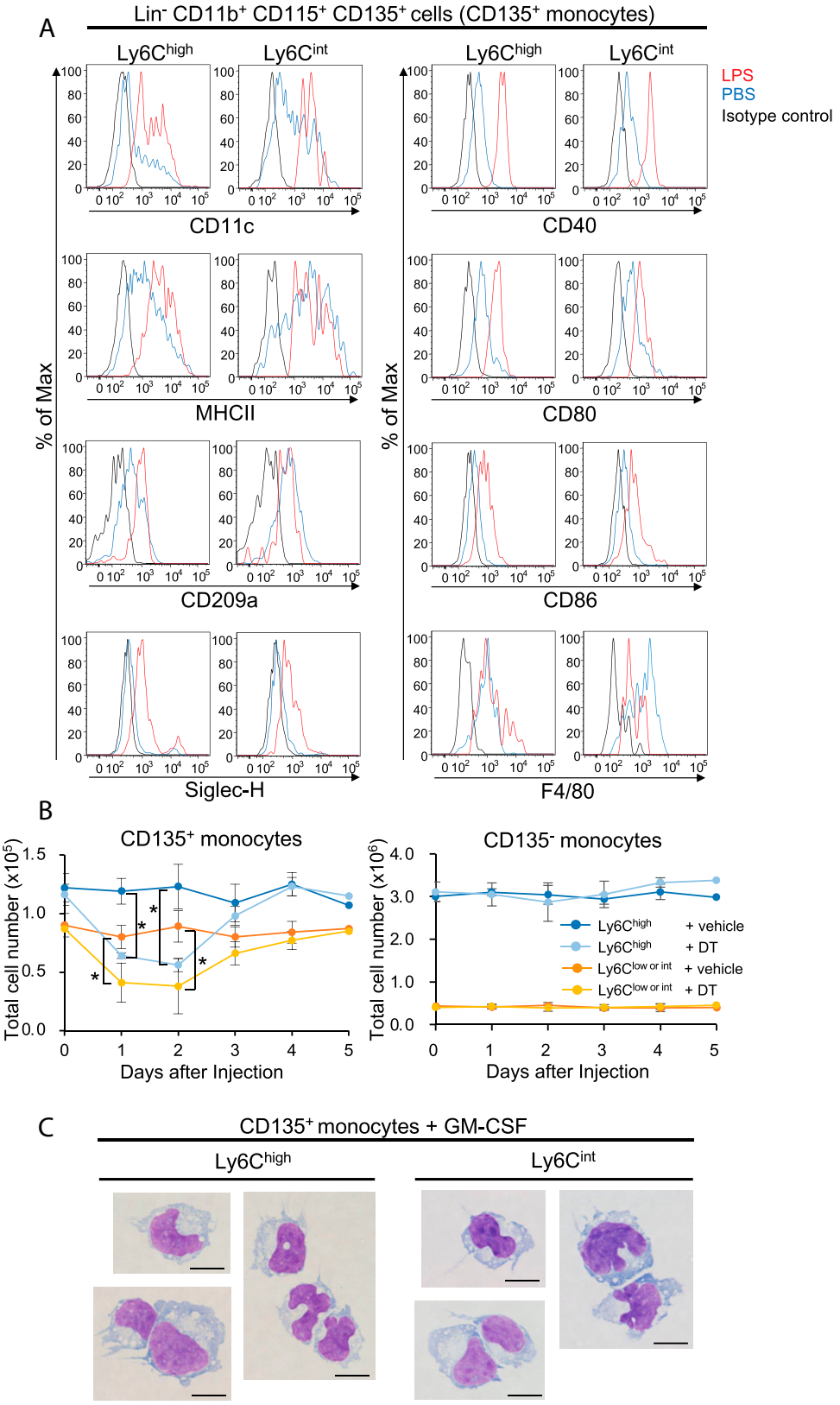

FIGURE 3. Expression of dendritic cell markers on CD135$^+$ monocytes. (**A**) Flow cytometric analysis of CD135$^+$ monocytes. Bone marrow cells were harvested from mice i.p. injected either with PBS or 5 μg of LPS 12 h prior to analysis. Black lines indicate isotype controls. (**B**) CD11c promoter–diphtheria toxin receptor (DTR) transgenic mice were treated either with vehicle or DT. The numbers of Ly6C^{high} and Ly6C^{int} CD135$^+$ monocytes (left panel) or Ly6C^{high} and Ly6C^{low} CD135$^-$ monocytes (right panel) in the bone marrow (BM) are shown. Data are means ± SD of three mice (*$p < 0.05$, determined by Student t test). (**C**) Giemsa staining of purified Ly6C^{high} and Ly6C^{int} CD135$^+$ monocytes after a 16-h incubation with recombinant mouse GM-CSF. Scale bars, 10 μm. Data are representative of at least six independent experiments.

CD135$^+$ monocytes function as APCs

We next analyzed the phagocytosis and Ag presentation abilities of these cells (Fig. 6). Since Ly6C^{high} and Ly6C^{int} CD135$^+$ monocytes share almost identical gene expression profiles, we considered them together, using CD135$^+$ monocytes for further functional analysis.

To evaluate phagocytotic activity, CD135$^+$ monocytes (BM), Ly6C^{high} and Ly6C^{low} CD135$^-$ monocytes (BM), cDCs (spleen), and pDCs (CD3$^-$CD19$^-$NK1.1$^-$CD11c^{int}B220$^+$ cells in spleen) were purified and incubated for an hour with *E. coli* labeled with pH-sensitive fluorescence (Fig. 6A, 6B). Ly6C^{high} and Ly6C^{low}

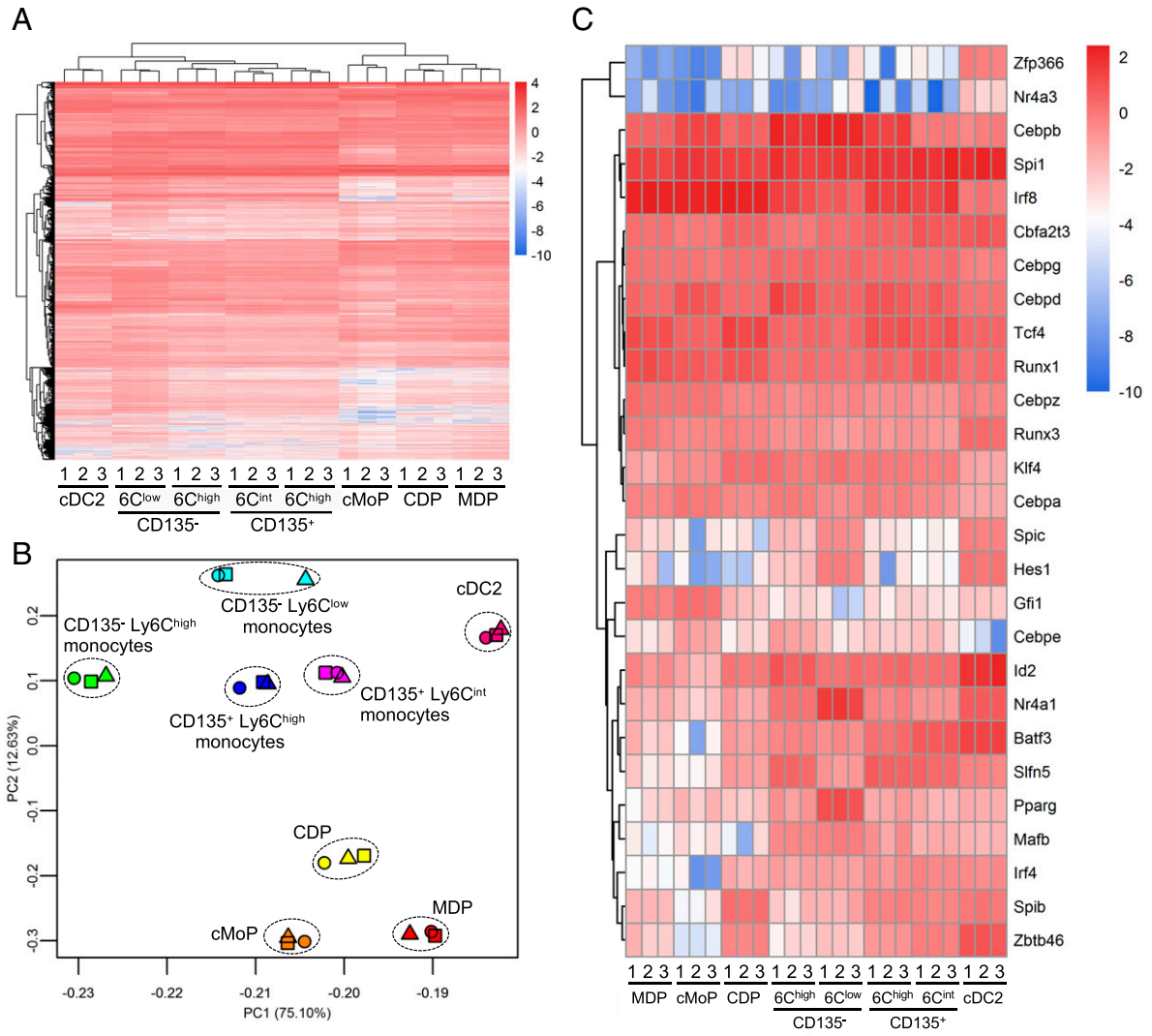

FIGURE 4. Transcriptional profiling of CD135$^+$ monocytes reveals their distinct identity. (**A** and **B**) Hierarchical tree clustering (A) and principal component analysis (B) of the normalized gene expression profiles of the indicated cells. (**C**) Heatmap of the mRNA expression of myeloid transcription factors in the indicated cells. 6C, Ly6C; cDC2, conventional dendritic cell type 2; CDP, common dendritic cell progenitor; cMoP, common monocyte progenitor; MDP, macrophage dendritic cell progenitor.

CD135$^-$ monocytes became fluorescence positive after the incubation, suggesting active phagocytosis and acidification of the phagosome. In contrast, cDCs and pDCs did not show any signs of phagocytosis or phagosome acidification under the same conditions. A marginal but statistically significant increase in the number of fluorescence-positive CD135$^+$ monocytes were detected, although fewer than of Ly6C^{high}CD135$^-$ monocytes. When sorted cells were subjected to longer preincubation on tissue culture plates and then to longer incubation with the labeled bacteria (2 h), cDCs revealed phagocytic activities and the phagocytic activity of CD135$^-$ monocytes was enhanced (Supplemental Fig. 4A). Even under this condition, CD135$^+$ monocytes showed phagocytic activities at an intermediate level between CD135$^-$ monocytes and cDCs. LPS did not enhance such phagocytic activity of Ly6C^{high} and Ly6C^{low} CD135$^-$ or CD135$^+$ monocytes (Fig. 6A, 6B).

For evaluation of Ag-presenting ability, we used an allogeneic MLR assay (50). Purified cells were cocultured with allogeneic CD4$^+$ T cells (Fig. 6C, 6D) or autologous (Fig. 6D) CD4$^+$ T cells that had been labeled with a fluorescent dye in advance. When allogeneic CD4$^+$ T cells were cocultured with cDCs for 4 d, a significant number of T cells with diluted fluorescence emerged, which indicates T cell proliferation in response to Ag presentation by cDCs (Fig. 6C, 6D). As expected, Ly6C^{high} and Ly6C^{low} CD135$^-$ monocytes failed to induce any T cell proliferation. In contrast, coculture with allogeneic CD135$^+$ monocytes resulted in proliferation of T cells, demonstrating their Ag-presenting ability (Fig. 6C, 6D). Proliferation index (the total number of divisions divided by the number of cells that went into division) for CD135$^+$ monocytes and cDCs was 1.96 ± 0.28 and 2.24 ± 0.21, respectively (mean ± SD, $p = 0.08$, $n = 6$ for CD135$^+$ monocytes and $n = 7$ for cDCs). Next, we evaluated the changes in the ability of Ag presentation and IFN-γ production in response to LPS (Fig. 6E–H). Allogeneic T cells stimulated by CD135$^+$ monocytes or cDCs proliferated (Fig. 6E, 6F) and produced IFN-γ (Fig. 6G, 6H). The Ag-presenting functions and IFN-γ production of cDCs and CD135$^+$ monocytes were not further enhanced by prestimulating them with LPS, suggesting that Ag presentation is a de novo function of these cells (Fig. 6E–H). These results clearly indicate that CD135$^+$ monocytes possess the ability to present Ags and stimulate T cell proliferation and induce IFN-γ production by the T cells.

Production of iNOS and TNF-α are the specific features common to Ly6C^{high} inflammatory monocytes and moDCs (49, 51). Indeed,

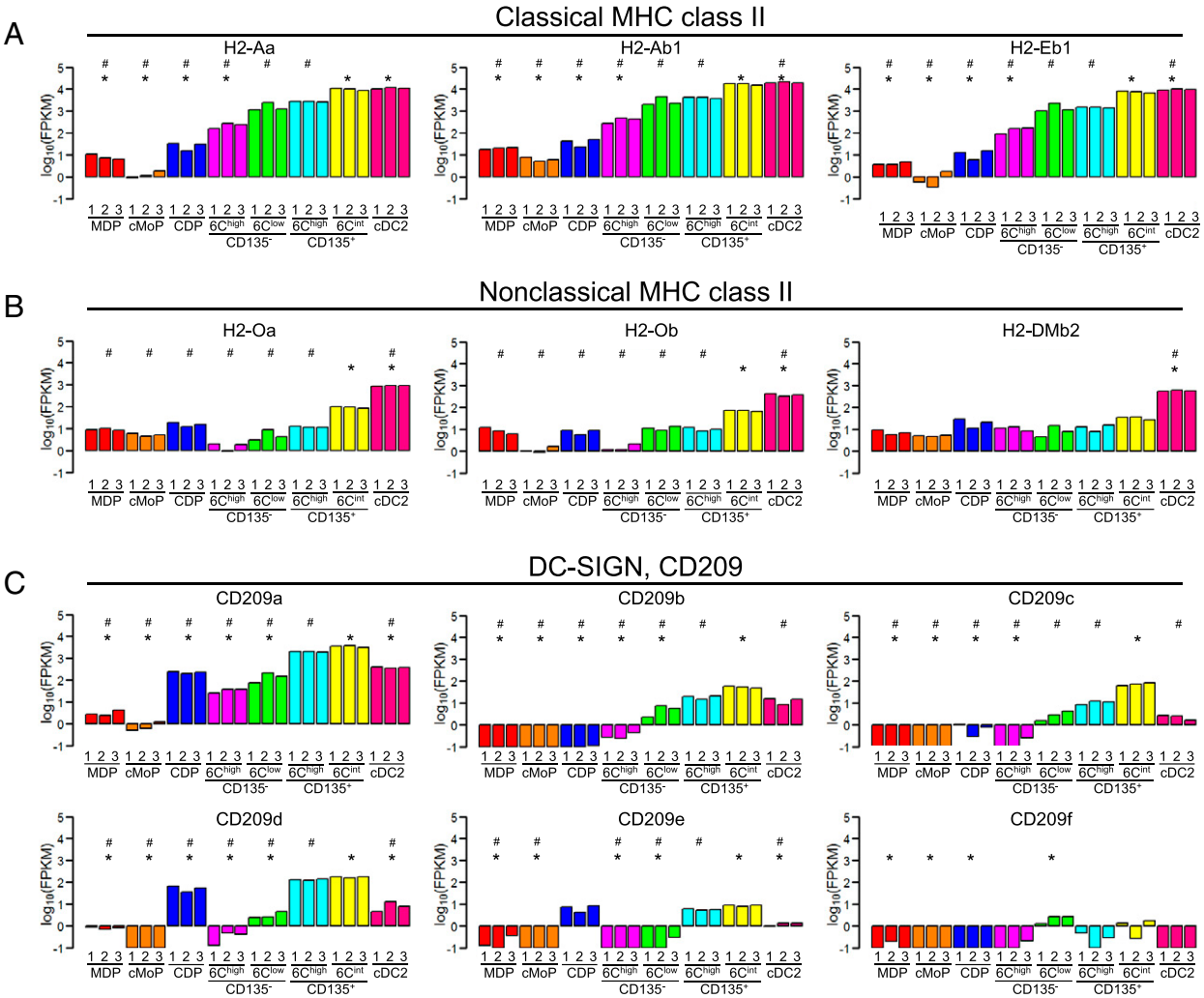

FIGURE 5. CD135$^+$ monocytes highly express MHC class II genes and Cd209 genes. (**A**–**C**) RNA expression of genes in the indicated cells are shown. $n = 3$ for each cell type. 6C, Ly6C; cDC2, conventional dendritic cell type 2; CDP, common dendritic cell progenitor; cMoP, common monocyte progenitor; MDP, macrophage dendritic cell progenitor. *$p < 0.05$ (comparison with Ly6C^{high}CD135$^+$ monocytes determined by the Tukey test); #$p < 0.05$ (comparison with Ly6C^{int}CD135$^+$ monocytes determined by the Tukey test).

we found that exposure of Ly6C^{high}CD135$^-$ monocytes to LPS induced iNOS and TNF-α production (Supplemental Fig. 4B–E). CD135$^+$ monocytes also produced iNOS and TNF-α in response to LPS, although at a lower level. Only a few cells of the Ly6C^{low}CD135$^-$ monocyte population expressed TNF-α. Neither cDCs nor pDCs produced iNOS or TNF-α regardless of the presence of LPS (Supplemental Fig. 4B–E).

CD135$^+$ monocytes are direct progeny of MDPs

We next sought to identify the differentiation pathway of CD135$^+$ monocytes. For this purpose, we used a CD45.1/CD45.2 congenic mouse system. In brief, MDPs, cMoPs, or CDPs (16–18) obtained from CD45.1 mice were injected directly into the tibial BM cavity of nonirradiated CD45.2 mice (Fig. 7). Flow cytometric analysis of BM and spleen cells of the recipient mice 60 and 108 h after the injection revealed that the donor-derived MDPs gave rise to CD135$^+$ monocytes in addition to CD115$^+$CD135$^+$ DCs and CD135$^-$ conventional monocytes (Fig. 7A, 7D, 7E). Although CDPs emerged in the BM and the spleen after MDP transfer, MDP-derived cMoPs were observed only in the BM, suggesting that BM is the optimal environment for cMoP development from MDPs (Fig. 7A, 7D). Then, we tested the differentiation potential of cMoPs and CDPs, which are direct progenitors of monocytes and DCs, respectively. In the recipients of cMoPs, the donor-derived cells were all CD135$^-$ monocytes, and no donor-derived CD135$^+$ monocytes were detected at both 60 and 108 h after the transfer (Fig. 7B, 7D, 7E). Consistent with a previous report (52), CDPs mostly differentiated into CD115$^+$CD135$^+$ DCs in the recipients (Fig. 7C, 7E). CDPs gave rise to cDCs in the spleen of the recipient less efficiently than MDPs (Fig. 7E). Although donor-derived CD135$^+$ monocytes were detectable in the recipients of CDPs, the contribution of CDPs as progenitors of CD135$^+$ monocytes was almost negligible because the recovery of CDP-derived cells in the recipients was very low (Fig. 7C, 7D, 7E). These results indicate that MDPs are the main and direct progenitors of CD135$^+$ monocytes and that CDPs poorly proliferate after transfer and the efficiency of differentiation from CDPs toward CD135$^+$ monocytes is much less than from MDPs.

CD135$^-$ monocytes do not give rise to CD135$^+$ monocytes

Accumulating evidence shows that moDCs are induced from monocytes under stress conditions or in vitro. In contrast, we have shown that CD135$^+$ monocytes, functioning as APCs such as DCs, readily exist at steady state. Then, we tested the upstream and downstream relationship between CD135$^-$ and CD135$^+$ monocytes using

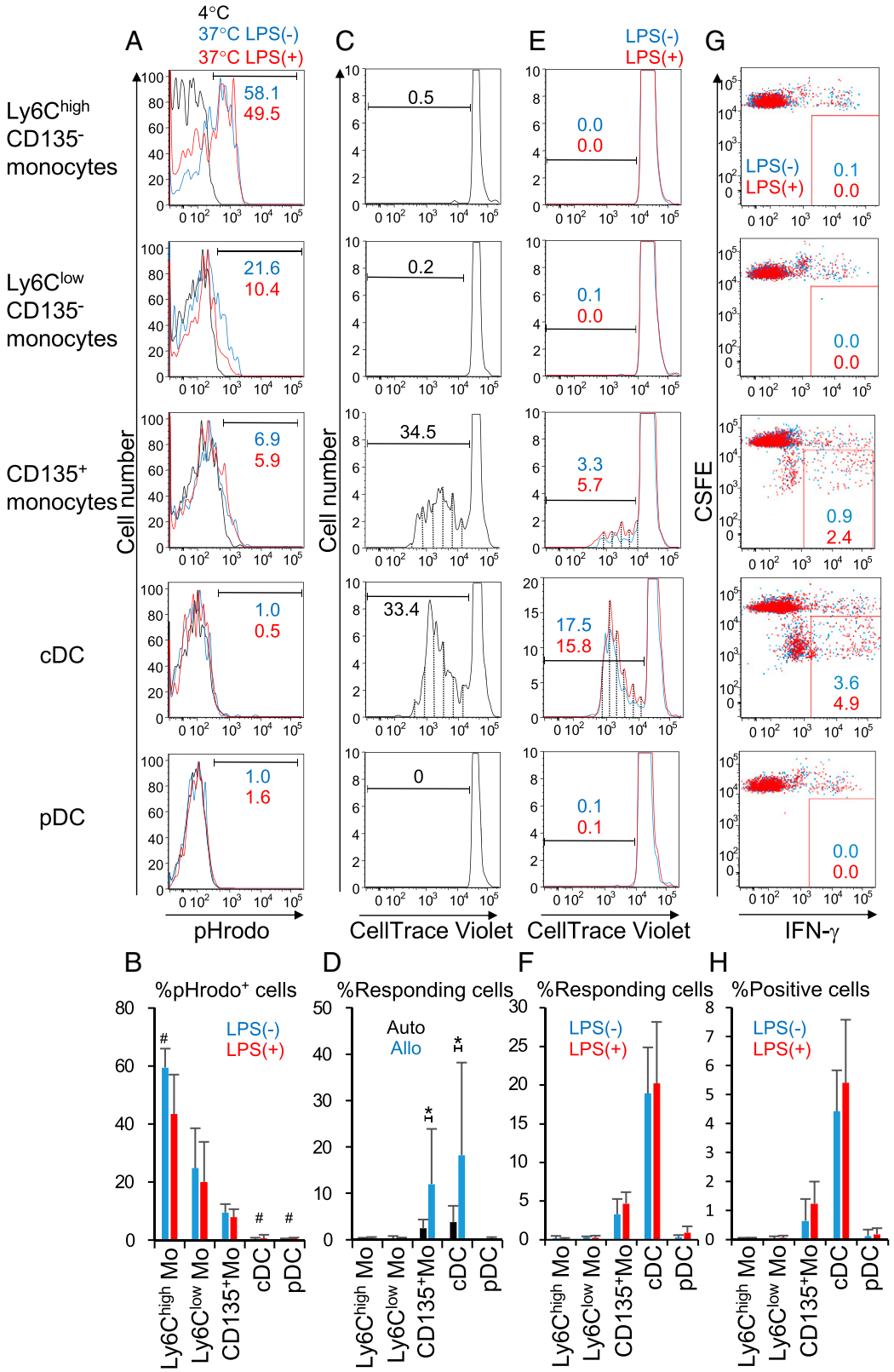

FIGURE 6. CD135$^+$ monocytes harbor the potential for phagocytosis and Ag presentation. (**A** and **B**) Phagocytic activity of the indicated cells was assessed using fluorescence-labeled bacteria (pHrodo). Purified cells were incubated for 2 h with or without LPS and then subjected to the phagocytosis assay. (**C** and **D**) Indicated cells were subjected to an autologous (Auto) or allogeneic (Allo) MLR assay. Flow cytometric analysis of allogeneic T cells cocultured with the indicated cells is shown in (C), and the frequencies of proliferating autologous or those of allogeneic T cells (cells with lower fluorescence than the control cells) are summarized in (D). Dotted lines in (C) indicate the peak position of each cell division. (**E**–**H**) IFN-γ production by the indicated cells (G and H) during the MLR using allogeneic T cells with or without prior LPS treatment (E and F). cDC, conventional dendritic cell; CDP, common dendritic cell progenitor; cMoP, common monocyte progenitor; MDP, macrophage dendritic cell progenitor; pDC, plasmacytoid dendritic cell. Dot plots and histograms are representatives of four to nine independent experiments. Dotted lines in (E) indicate the peak position of each cell division. Data are means ± SD of four to nine independent experiments ($^{\#}p < 0.05$ comparison with between LPS(−) and LPS(+); $^{*}p < 0.05$, comparison between autologous and allogeneic reactions determined by Student *t* test).

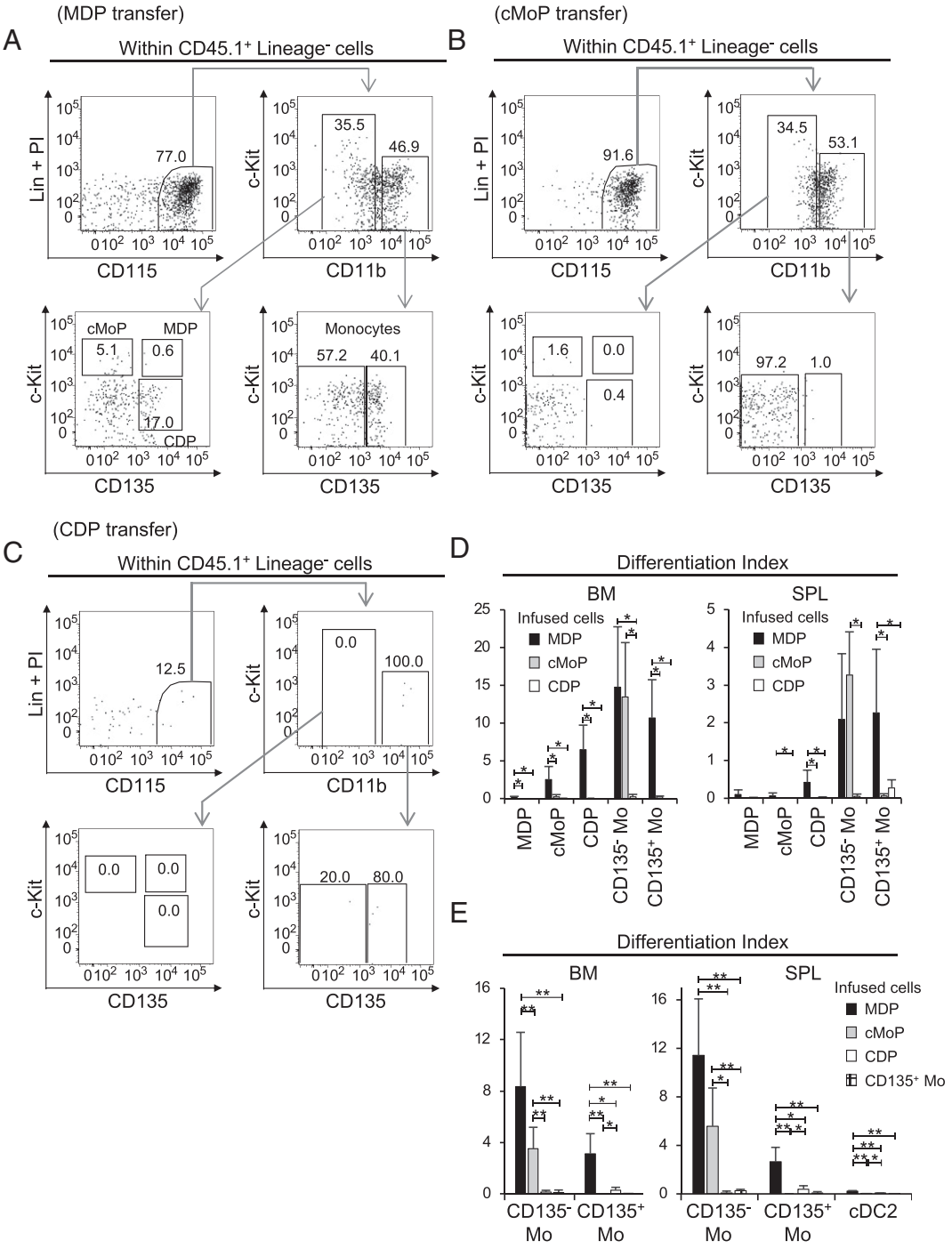

FIGURE 7. CD135$^+$ monocytes are mostly derived from MDPs. (**A–C**) Representative flow cytometric analysis of bone marrow (BM) cells of CD45.2 recipient mice that had been adoptively transferred with (A) macrophage dendritic cell progenitors (MDPs), (B) common monocyte progenitors (cMoPs), or (C) common dendritic cell progenitors (CDPs) obtained from the BM of CD45.1 mice. (**D**) Flow cytometric analysis summary of BM cells or spleen (SPL) of CD45.2 recipient mice 60 h after respective transfers. Mo, monocytes. (**E**) Summary of flow cytometric analysis of BM cells or SPL cells of CD45.2 recipient mice 108 h after respective transfers of MDP, cMoP, CDP, or CD135$^+$ Mo. Differentiation index was defined as (% in donor-derived indicated cells in tibial BM cells/the number of infused cells) $\times 10^8$, which is supposed to reflect the differentiation efficiency of the infused cells. Data are means ± SD of six independent experiments (for D) or four independent experiments (for E). ($*p < 0.05$, $**p < 0.01$, determined by Student t test).

adoptive transfer experiments with the CD45.1/CD45.2 congenic mouse system. Ly6C^{high}CD135$^-$ monocytes, Ly6C^{low}CD135$^-$ monocytes, or CD135$^+$ monocytes were purified from BM cells and then adoptively transferred into the tibial BM cavity of nonirradiated mice as mentioned above (Fig. 8). In the recipients of Ly6C^{high}CD135$^-$ monocytes, donor-derived cells were detected in both Ly6C^{high} and Ly6C^{low} CD135$^-$ monocytes as previously reported (53, 54), but not in CD135$^+$ monocytes. Ly6C^{low}CD135$^-$ monocytes gave rise only to Ly6C^{low}CD135$^-$ monocytes. CD135$^+$ monocytes did not differentiate into either Ly6C^{high} or Ly6C^{low} CD135$^-$ monocytes (Fig. 8) or cDCs (Fig. 7E) in the recipients. These results were consistent with our finding that cMoPs did not

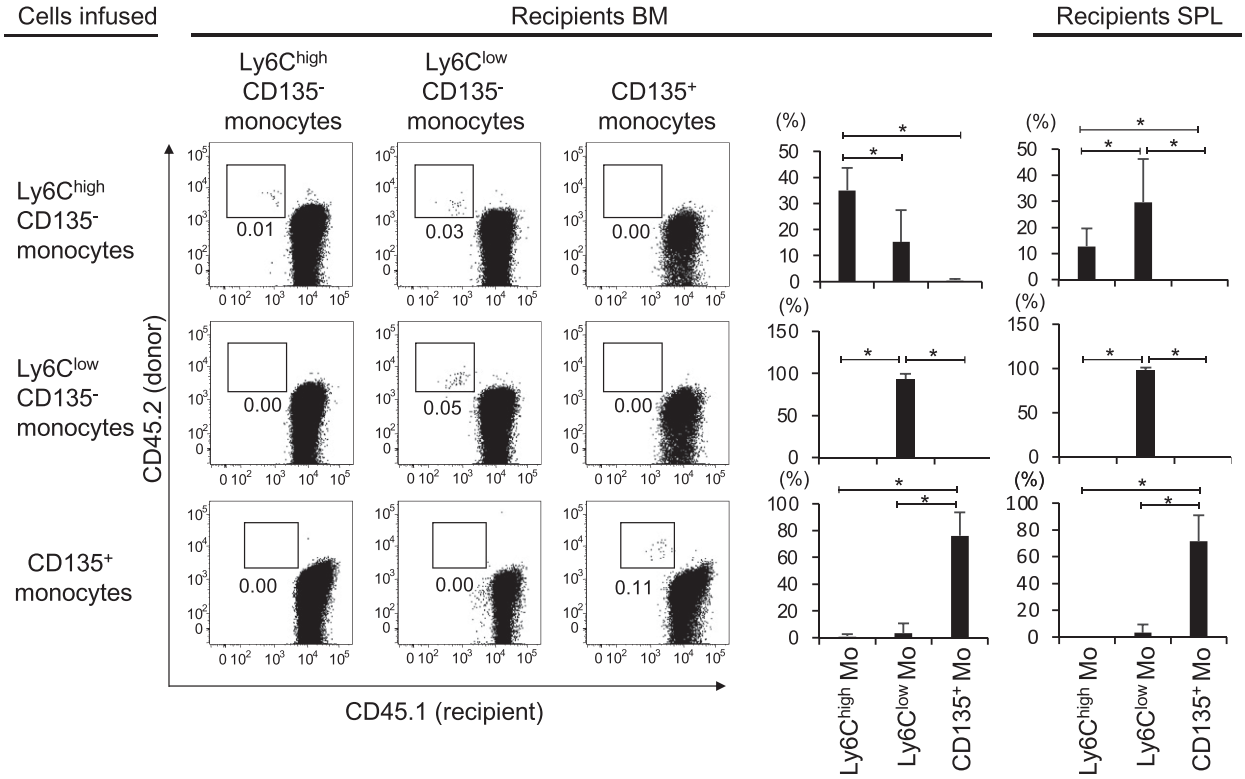

FIGURE 8. CD135$^+$ monocytes are neither progenitors nor progeny of CD135$^-$ monocytes. Flow cytometric analysis of bone marrow (BM) or spleen (SPL) of CD45.1 recipient mice that had been adoptively transferred with Ly6C^{high} or Ly6C^{low} CD135$^-$ monocytes (Mo) or CD135$^+$ Mo obtained from the BM of CD45.2 donor mice. The numbers are frequencies of donor-derived cells among the indicated cells in the recipients. Bar graphs indicate the frequencies among donor-derived CD11b$^+$CD115$^+$ monocytes. Dot plots are representatives of four to eight independent experiments. Data are means ± SD of four to eight independent experiments. (*$p < 0.05$, determined by Student t test).

give rise to CD135$^+$ monocytes, and they clearly demonstrate that the differentiation pathway of CD135$^+$ monocytes is distinct from that of conventional monocytes.

Discussion

In this study, we have identified CD135$^+$ monocytes as novel APCs in the mouse. They are morphologically similar to classical monocytes, found in BM, spleen, and PB at steady state, and express surface markers specific to DCs, in addition to monocytic markers including CD115 and CD11b, which are the hallmarks of mouse monocytes (35, 53). In addition to the phenotypical resemblance to DCs, these CD135$^+$ monocytes are equipped with the ability to phagocytose external Ags and to activate naive T lymphocytes.

In this study, we identified and characterized a CD135$^+$ subpopulation within mouse CD115$^+$CD11b$^+$ monocytes. Moreover, we redefined Ly6C^{high} and Ly6C^{low} conventional monocytes (33, 55) within the CD135$^-$ monocytes. The gene expression profile findings support CD135$^+$ monocytes having a distinct identity among known cells within the MPS. We found that Ly6C expression on CD135$^+$ monocytes ranged from intermediate to high levels in a continuous manner and, although Ly6C^{int} cells expressed higher levels of DC signature molecules, such as MHC class II and CD11c, there were no other significant differences between the gene expression profiles of Ly6C^{high} and Ly6C^{int} cells. Thus, we consider that they are almost identical. In CD135$^+$ monocytes, MHC class II genes were highly expressed at a level almost equivalent to that in cDC2s. To our surprise, CD209 genes known as DC-SIGNs were expressed at the highest levels in all the analyzed cells. These features of CD135$^+$ monocytes reflected their function as APCs demonstrated by our analysis.

CD135$^+$ monocytes exhibit properties of both monocytes and DCs. These features remind us of those of moDCs (1, 7, 9, 13, 14, 49). Typically, moDCs do not exist at steady state but are induced from monocytes under inflammatory conditions, including various infections or GM-CSF stimulation in vitro (7, 48, 56). During the induction of moDCs, monocytes acquire expression of general DC markers including CD11c and MHC class II. In contrast, the CD135$^+$ monocytes in our study existed readily at steady state and expressed DC markers, suggesting that they are different from moDCs. As revealed by others, conventional monocytes are heterogeneous in both mice and humans, and mouse monocytes are classified according to their Ly6C expression level (14, 31, 55). Interestingly, candidates for moDCs precursors have been identified within a Ly6C^{int} subset (35). In another report, surface MHC class II$^-$ (intracellular MHC class II$^+$) CD11c$^-$CD209a$^+$Ly6C^{high} monocytes are shown as precursors of moDCs, giving rise to moDCs in response to GM-CSF and being independent of Flt3L (57). CD135$^+$ monocytes in our study similarly expressed CD209a at a high level, but they also expressed CD11c and MHC class II on their surface. Furthermore, our results demonstrated that differentiation of CD135$^+$ monocytes was clearly dependent on Flt3L. These results suggest that CD135$^+$ monocytes are not identical to known precursors of moDCs. In addition, analysis in the steady state showed that intra-BM transfer of Ly6C^{high} CD135$^-$ monocytes or CD135$^+$ monocytes did not result in the emergence of the other population, suggesting that these cells are mutually distinct. These results strongly suggest that CD135$^+$ monocytes are novel de novo APCs that exist at steady state. Further studies are needed to investigate

the possibility that CD135$^+$ monocytes are some forms of moDCs, and/or that moDCs are independently derived from CD135$^-$ monocytes under inflammatory conditions.

CD135$^+$ monocytes have similarities with other cells within MPS. Menezes et al. (57) identified R2 and R3 cells within a CD135$^+$CD115$^+$ cellular fraction. CD135$^+$ monocytes are also similar to pre-cDC2s as found by Schlitzer et al. (58). Pre-cDC2s expressed CD135 and Ly6C. However, R2, R3 cells, and pre-cDC2s were defined within the MHC class II$^-$ population, whereas most CD135$^+$ monocytes expressed MHC class II, as shown in Fig. 3A. In addition, R2 cells were negative for CD11C, which is expressed by CD135$^+$ monocytes. Functionally, transfer of CD135$^+$ monocytes did not give rise to cDC2s in the spleen of the recipients (Fig. 7E). Yáñez et al. also identified CD135-expressing cells within CD11b$^+$CD115$^+$ cells (15). However, they were negative for Ly6C and F4/80, both of which were expressed by CD135$^+$ monocytes (Figs. 1A and 3A, respectively). Although we cannot completely rule out the possibility of some overlaps, we have currently concluded that CD135$^+$ monocytes are different from those cells reported by others. Monocytes, macrophages, and DCs, all members of the MPS, share many properties, gene expression profiles, and differentiation pathways (13, 49). Given that CD135$^+$ monocytes are classified as monocytes, we expected that they would be descendants of cMoPs, as cMoPs are considered to be progenitors with limited potential to differentiate into all kinds of monocytes (18). Indeed, we verified that Ly6C^{high} and Ly6C^{low} CD135$^+$ conventional monocytes were derived from cMoPs. However, the vast majority of CD135$^+$ monocytes were differentiated directly from MDPs but never from cMoPs, to our surprise. Considering that CD135$^+$ monocytes have the ability to present Ags even at steady state and have a unique differentiation pathway, it might be better to avoid referring to them as monocytes and instead name them "monocytoid DCs."

Development of cellular components of the MPS is governed by complex networks of transcriptional regulation, and cell type–specific requirements for transcription factors have been identified such as *Klf4* and *Irf8* for Ly6C^{high} monocytes, and *Nr4a1* and *Cebpb* for Ly6C^{low} monocytes (35, 59–62). We have not identified any specific transcription factors required for the development of CD135$^+$ monocytes so far. However, RNA-seq analysis revealed that CD135$^+$ monocytes expressed *Irf8* at a higher level than CD135$^-$ conventional monocytes or cDC2s. Because Ly6C^{high} monocytes (including both CD135$^-$ and CD135$^+$) are markedly reduced in *Irf8*-deficient mice (62), we hypothesize that Irf8 plays important roles in specification, differentiation, or maintenance of CD135$^+$ monocytes in addition to its known roles in other monocytes and DCs (62, 63). We are currently investigating the molecular mechanisms that regulate the supply of CD135$^+$ monocytes.

In summary, our results clearly showed the existence of a novel APC population with a distinct differentiation pathway among monocytes. CD135$^+$ monocytes are circulating through lymphoid organs and PB in the steady state with the abilities to activate naive T cells by presenting Ags, indicating that they play an important role in protecting homeostasis from external Ags through their immune functions. Recently, novel DCs/DC-like cells have been identified in human PB as well (64–66). Redefinition of conventional monocytes as a CD135$^-$ subset should be also of great impact on our understanding of MPS. We are currently working to further elucidate the differentiation and functions of CD135$^+$ monocytes under healthy and diseased condition with the aim of better understanding the MPS complex and the immune responses.

Acknowledgments

We thank Dr. Shigekazu Nagata (Osaka University) for providing CD45.1 mice. We thank Drs. Hiroshi Kawamoto, Junji Uehori and Yosuke Nagahata (Kyoto University) for technical advice. We are also grateful to Yoko Nakagawa for excellent technical assistance.

Disclosures

The authors have no financial conflicts of interest.

References

1. Mildner, A., and S. Jung. 2014. Development and function of dendritic cell subsets. *Immunity* 40: 642–656.
2. Merad, M., P. Sathe, J. Helft, J. Miller, and A. Mortha. 2013. The dendritic cell lineage: ontogeny and function of dendritic cells and their subsets in the steady state and the inflamed setting. *Annu. Rev. Immunol.* 31: 563–604.
3. Steinman, R. M., and J. Idoyaga. 2010. Features of the dendritic cell lineage. *Immunol. Rev.* 234: 5–17.
4. Murphy, T. L., G. E. Grajales-Reyes, X. Wu, R. Tussiwand, C. G. Briseño, A. Iwata, N. M. Kretzer, V. Durai, and K. M. Murphy. 2016. Transcriptional control of dendritic cell development. *Annu. Rev. Immunol.* 34: 93–119.
5. Nakano, H., M. Yanagita, and M. D. Gunn. 2001. CD11c$^+$B220$^+$Gr-1$^+$ cells in mouse lymph nodes and spleen display characteristics of plasmacytoid dendritic cells. *J. Exp. Med.* 194: 1171–1178.
6. Chapuis, F., M. Rosenzwajg, M. Yagello, M. Ekman, P. Biberfeld, and J. C. Gluckman. 1997. Differentiation of human dendritic cells from monocytes in vitro. *Eur. J. Immunol.* 27: 431–441.
7. Segura, E., and S. Amigorena. 2013. Inflammatory dendritic cells in mice and humans. *Trends Immunol.* 34: 440–445.
8. Mildner, A., S. Yona, and S. Jung. 2013. A close encounter of the third kind: monocyte-derived cells. *Adv. Immunol.* 120: 69–103.
9. León, B., M. López-Bravo, and C. Ardavín. 2007. Monocyte-derived dendritic cells formed at the infection site control the induction of protective T helper 1 responses against *Leishmania. Immunity* 26: 519–531.
10. Rodrigues, P. F., L. Alberti-Servera, A. Eremin, G. E. Grajales-Reyes, R. Ivanek, and R. Tussiwand. 2018. Distinct progenitor lineages contribute to the heterogeneity of plasmacytoid dendritic cells. *Nat. Immunol.* 19: 711–722.
11. Guiducci, C., R. L. Coffman, and F. J. Barrat. 2009. Signalling pathways leading to IFN-α production in human plasmacytoid dendritic cell and the possible use of agonists or antagonists of TLR7 and TLR9 in clinical indications. *J. Intern. Med.* 265: 43–57.
12. Siegal, F. P., N. Kadowaki, M. Shodell, P. A. Fitzgerald-Bocarsly, K. Shah, S. Ho, S. Antonenko, and Y. J. Liu. 1999. The nature of the principal type 1 interferon-producing cells in human blood. *Science* 284: 1835–1837.
13. Guilliams, M., F. Ginhoux, C. Jakubzick, S. H. Naik, N. Onai, B. U. Schraml, E. Segura, R. Tussiwand, and S. Yona. 2014. Dendritic cells, monocytes and macrophages: a unified nomenclature based on ontogeny. *Nat. Rev. Immunol.* 14: 571–578.
14. Guilliams, M., A. Mildner, and S. Yona. 2018. Developmental and functional heterogeneity of monocytes. *Immunity* 49: 595–613.
15. Yáñez, A., S. G. Coetzee, A. Olsson, D. E. Muench, B. P. Berman, D. J. Hazelett, N. Salomonis, H. L. Grimes, and H. S. Goodridge. 2017. Granulocyte-monocyte progenitors and monocyte-dendritic cell progenitors independently produce functionally distinct monocytes. *Immunity* 47: 890–902.e4.
16. Fogg, D. K., C. Sibon, C. Miled, S. Jung, P. Aucouturier, D. R. Littman, A. Cumano, and F. Geissmann. 2006. A clonogenic bone marrow progenitor specific for macrophages and dendritic cells. *Science* 311: 83–87.
17. Onai, N., A. Obata-Onai, M. A. Schmid, T. Ohteki, D. Jarrossay, and M. G. Manz. 2007. Identification of clonogenic common Flt3$^+$M-CSFR$^+$ plasmacytoid and conventional dendritic cell progenitors in mouse bone marrow. *Nat. Immunol.* 8: 1207–1216.
18. Hettinger, J., D. M. Richards, J. Hansson, M. M. Barra, A. C. Joschko, J. Krijgsveld, and M. Feuerer. 2013. Origin of monocytes and macrophages in a committed progenitor. *Nat. Immunol.* 14: 821–830.
19. Karsunky, H., M. Merad, A. Cozzio, I. L. Weissman, and M. G. Manz. 2003. Flt3 ligand regulates dendritic cell development from Flt3$^+$ lymphoid and myeloid-committed progenitors to Flt3$^+$ dendritic cells in vivo. *J. Exp. Med.* 198: 305–313.
20. Miller, J. C., B. D. Brown, T. Shay, E. L. Gautier, V. Jojic, A. Cohain, G. Pandey, M. Leboeuf, K. G. Elpek, J. Helft, et al.; Immunological Genome Consortium. 2012. Deciphering the transcriptional network of the dendritic cell lineage. *Nat. Immunol.* 13: 888–899.
21. Waskow, C., K. Liu, G. Darrasse-Jèze, P. Guermonprez, F. Ginhoux, M. Merad, T. Shengelia, K. Yao, and M. Nussenzweig. 2008. The receptor tyrosine kinase Flt3 is required for dendritic cell development in peripheral lymphoid tissues. *Nat. Immunol.* 9: 676–683.
22. Romani, N., S. Gruner, D. Brang, E. Kämpgen, A. Lenz, B. Trockenbacher, G. Konwalinka, P. O. Fritsch, R. M. Steinman, and G. Schuler. 1994. Proliferating dendritic cell progenitors in human blood. *J. Exp. Med.* 180: 83–93.
23. Shortman, K., and S. H. Naik. 2007. Steady-state and inflammatory dendritic-cell development. *Nat. Rev. Immunol.* 7: 19–30.
24. Rivollier, A., J. He, A. Kole, V. Valatas, and B. L. Kelsall. 2012. Inflammation switches the differentiation program of Ly6C^{hi} monocytes from antiinflammatory

macrophages to inflammatory dendritic cells in the colon. *J. Exp. Med.* 209: 139–155.
25. Zigmond, E., C. Varol, J. Farache, E. Elmaliah, A. T. Satpathy, G. Friedlander, M. Mack, N. Shpigel, I. G. Boneca, K. M. Murphy, et al. 2012. Ly6C ^{hi} monocytes in the inflamed colon give rise to proinflammatory effector cells and migratory antigen-presenting cells. *Immunity* 37: 1076–1090.
26. Greter, M., J. Helft, A. Chow, D. Hashimoto, A. Mortha, J. Agudo-Cantero, M. Bogunovic, E. L. Gautier, J. Miller, M. Leboeuf, et al. 2012. GM-CSF controls nonlymphoid tissue dendritic cell homeostasis but is dispensable for the differentiation of inflammatory dendritic cells. *Immunity* 36: 1031–1046.
27. Posch, W., C. Lass-Flörl, and D. Wilflingseder. 2016. Generation of human monocyte-derived dendritic cells from whole blood. *J. Vis. Exp.* 118: 54968.
28. Zarif, J. C., J. R. Hernandez, J. E. Verdone, S. P. Campbell, C. G. Drake, and K. J. Pienta. 2016. A phased strategy to differentiate human CD14^{+}monocytes into classically and alternatively activated macrophages and dendritic cells. *Biotechniques* 61: 33–41.
29. Anguille, S., E. L. Smits, E. Lion, V. F. van Tendeloo, and Z. N. Berneman. 2014. Clinical use of dendritic cells for cancer therapy. *Lancet Oncol.* 15: e257–e267.
30. Palucka, K., and J. Banchereau. 2013. Dendritic-cell-based therapeutic cancer vaccines. *Immunity* 39: 38–48.
31. Wong, K. L., J. J. Tai, W. C. Wong, H. Han, X. Sem, W. H. Yeap, P. Kourilsky, and S. C. Wong. 2011. Gene expression profiling reveals the defining features of the c

Supplemental Table 1 Antibodies used for flow cytometry

Antigen	Clone	Fluorochrome	Source
CD11b	M1/70	FITC	BioLegend
		PE-Cy7	BD biosciences
CD135	A2F10	PE, biotin	BioLegend
CD115	AFS98	APC	BioLegend
		VioBright, FITC	Miltenyi Biotec
c-kit	2B8	APC-Cy7	BioLegend
Ly6C	AL-21	V450	BD biosciences
CD11c	HL3	FITC, PE	BD biosciences
B220	RA3-6B2	APC	BD biosciences
I-A/I-E	M5/114.15.2	FITC	eBioscience
F4/80	BM8	FITC	eBioscience
		PE	BioLegend
CD16/32	93	APC	eBioscience
PD-L1	10F.9G2	APC	BioLegend
PD-L2	TY25	APC	BioLegend
CD40	FGK45.5	FITC	Miltenyi Biotec
CD80	16-10A1	FITC	eBioscience
CD86	GL-1	FITC	TONBO bioscience
SiglecH	eBio440c	FITC	eBioscience
SIRPα	P84	APC	BioLegend
CD45.1	A20	FITC, V450	BD biosciences
CD45.2	104	FITC	eBioscience
		APC-Cy7	BD biosciences
CD206	C068C2	APC	BioLegend
CD301a	LOM-8.7	AlexaFluor647	BioLegend
CD64	16E2	PE	BioLegend
CCR2	X54-5/7.1	PE	BioLegend
CD3	17A2	PerCP-Cy5.5	BioLegend
CD19	1D3	PerCP-Cy5.5	BD biosciences
NK1.1	PK136	PerCP-Cy5.5	TONBO bioscience
Ter119	Ter-119	PerCP-Cy5.5	BD biosciences
Ly6G	1A8	PerCP-Cy5.5	BioLegend
CD209a	LWC06	APC	invitrogen
iNOS	CXNFT	APC	invitrogen
IFNγ	XMG1.2	AlexaFluor647	BD biosciences
TNF	MP6-XT22	AlexaFluor647	BD biosciences

Supplemental Figure 1

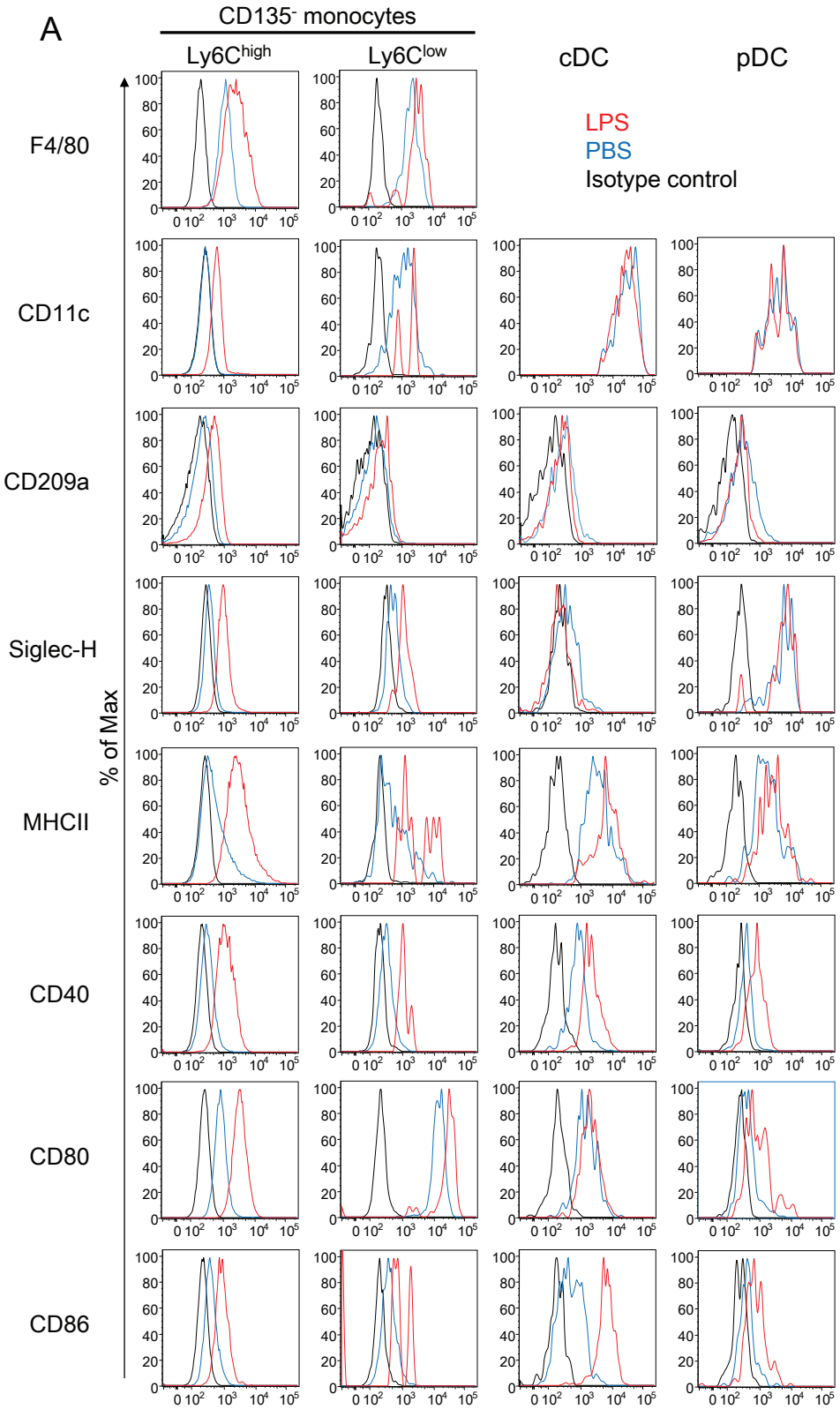

Supplemental Figure 1: **Expression of markers specific for macrophages and dendritic cells by CD135- monocytes and dendritic cells**

Flow cytometric analysis of CD135- monocytes and conventional dendritic cells (cDC) and plasmacytoid dendritic cells (pDC). Bone marrow monocytes or spleen cDCs and pDCs were harvested from mice treated either with phosphate buffered saline (PBS) or lipopolysaccharide (LPS). Black lines indicate isotype controls.

Supplemental Figure 2

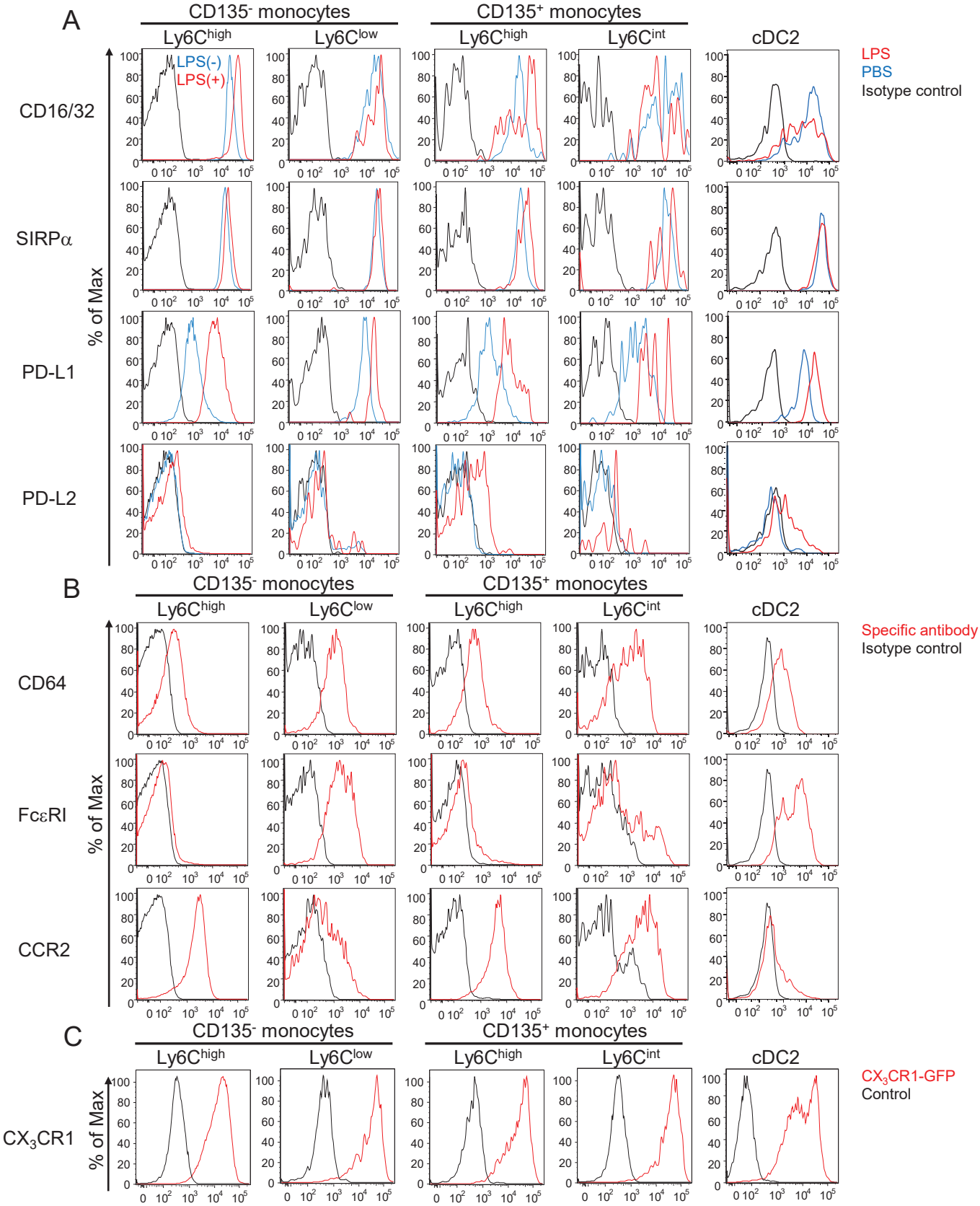

Supplemental Figure 2: **Flow cytometric analysis of CD135$^+$ and CD135$^-$ monocytes and conventional dendritic cells 2 (cDC2) for expression of myeloid and monocytic markers**

(A) Bone marrow (BM) cells were harvested from mice treated either with phosphate buffered saline (PBS) (LPS (-)) or LPS (LPS (+)), and were subjected to flow cytometric analysis. Black lines indicate isotype controls. (B) and (C) BM cells were harvested from wild-type mice (B) or CX_3CR1-GFP mice (C) and were subjected to flow cytometric analysis. Black lines indicate isotype (B) or wild-type (C) controls. Data are representative of at least three independent experiments.

Supplemental Figure 3

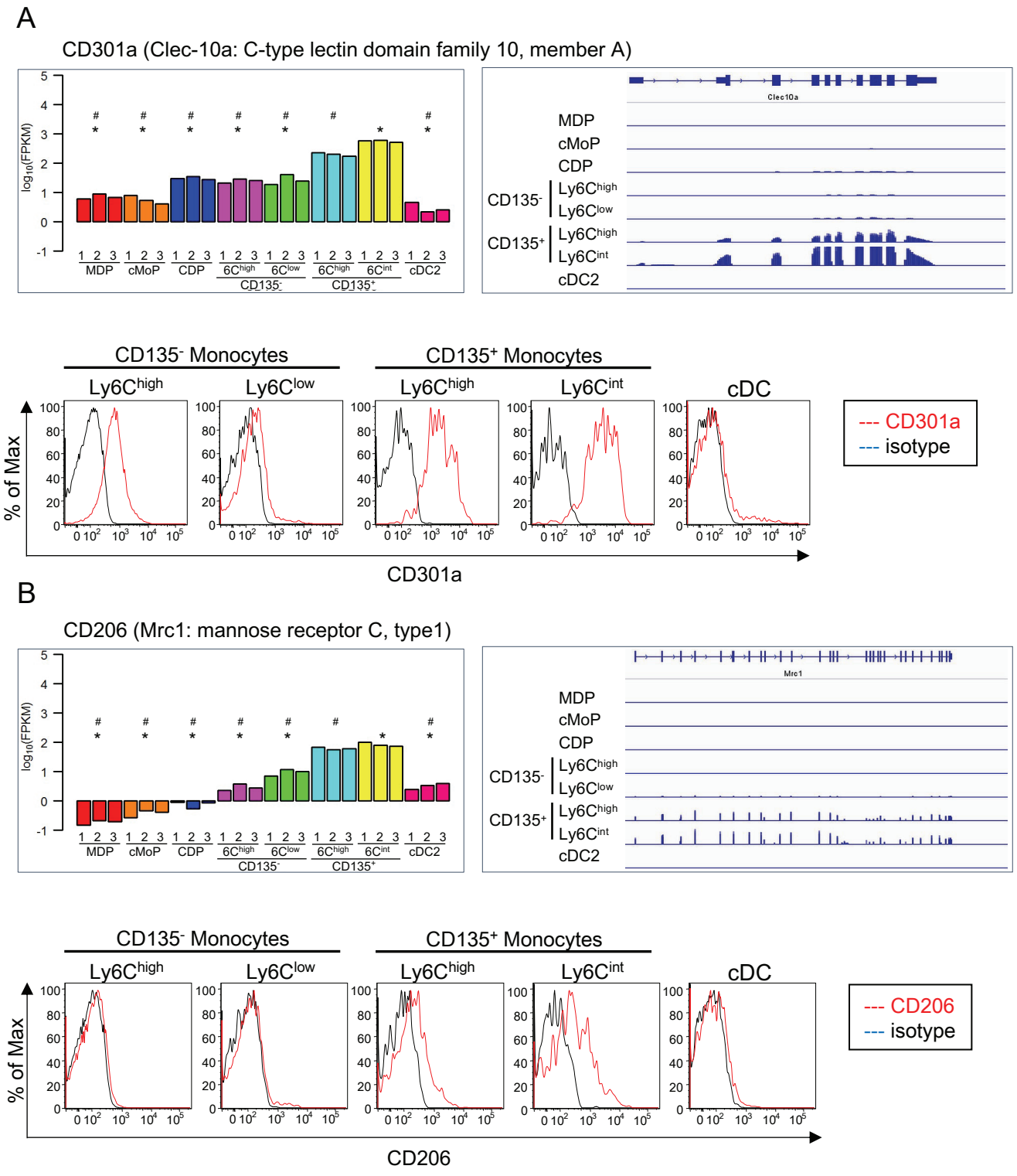

Supplemental Figure 3: **CD135^{+} monocytes specifically express *Cd301a* and *Cd206* genes**
(A) mRNA and cell surface expression of Cd301a and (B) Cd206 in the indicated cells are shown. N=3 for each cell type. MDP, macrophage dendritic cell progenitor; cMoP, common monocyte progenitor; CDP, common dendritic cell progenitor; cDC2, conventional dendritic cell type 2; 6C, Ly6C. *, $p<0.05$ (comparison with Ly6C^{high} CD135^{+} monocytes determined by the Tukey test); #, $p<0.05$ (comparison with Ly6C^{int} CD135^{+} monocytes determined by the Tukey test).

Supplemental Figure 4

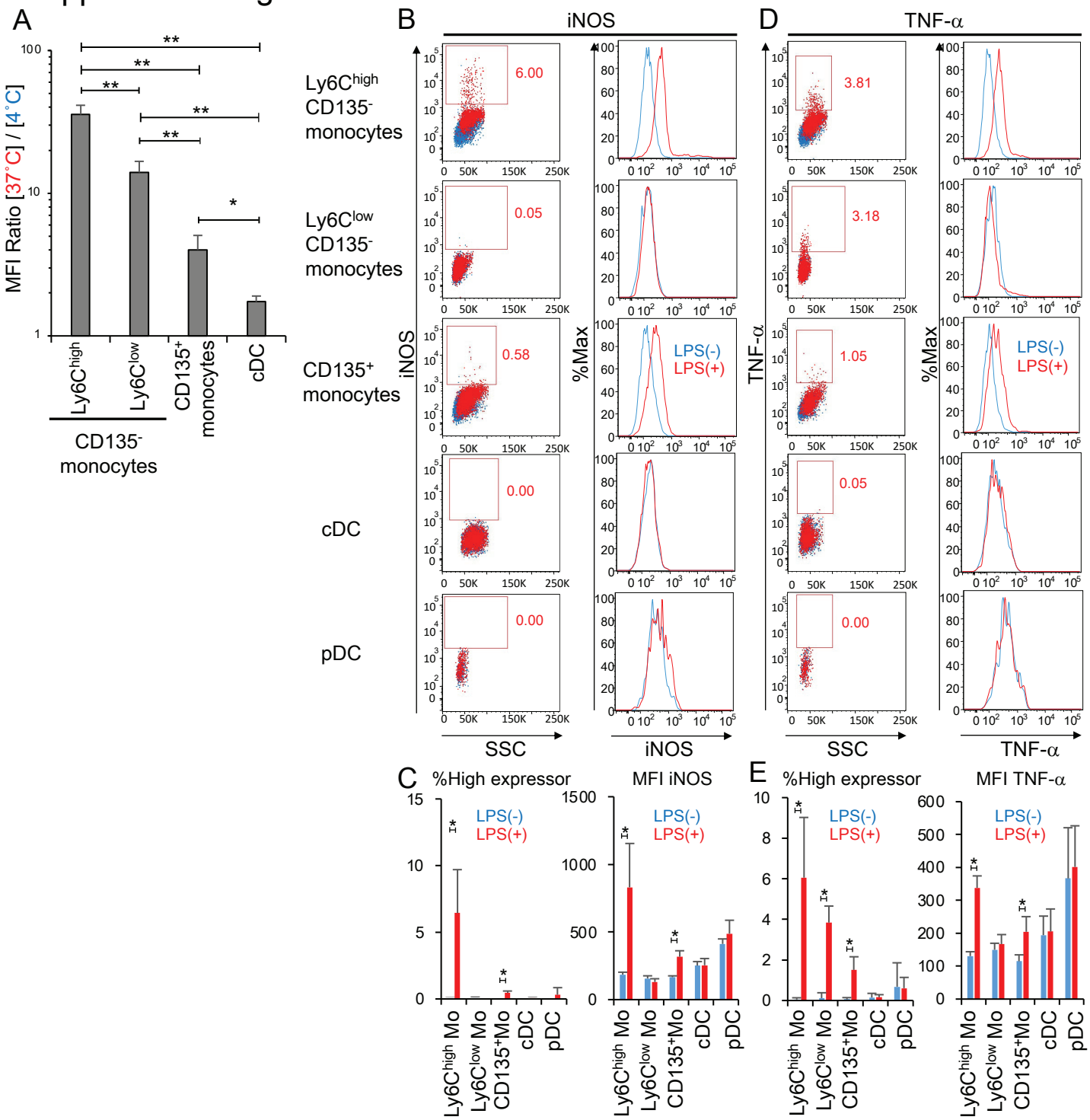

Supplemental Figure 4: **Functions of CD135$^+$ and CD135$^-$ monocytes and conventional dendritic cells (cDC)**
(A) Phagocytic activities. Indicated cells were sorted from pooled mouse bone marrow and spleen cells, and resuspended in IMDM culture medium (Wako, Osaka, Japan) supplemented with 15% FCS and 1% GlutaMax (Gibco, NY, USA). After 2 hours-preculture in tissue culture treated flat-bottomed 96-well plates in a CO_2 incubator and subsequent incubation on ice for 10 min, cells were further incubated in the presence of pHrodo Red *E. coli* BioParticles Conjugate for Phagocytosis (Invitrogen, Carlsbad, CA) either at 4°C or 37°C for 2 hours. These cells were directly analyzed by flow cytometry after adding 7-AAD. The ratio of mean fluorescence intensity (MFI) of the cells incubated at 37°C to that at 4°C was calculated. The value > 1 indicates active phagocytosis. Data are means ± S.D. of four (CD135$^-$ Ly6C^{high} monocytes) or three (other cell types) independent experiments. (B-E) Production iNOS and TNF-α in response to LPS. The indicated cells were purified and incubated for 16 hours in the presence or absence of 1 μg/mL LPS prior to intracellular flow cytometric analysis of induced nitric oxide synthase (iNOS; B and C) or tumor necrosis factor-α (TNF-α; D and E). Dot plots are representatives of three to six independent experiments. High expressors are defined as cells with mean fluorescent intensity (MFI) > 2×10^3. Data are means ± S.D. of three to six independent experiments. experiments (*, $p<0.05$ and **, $p<0.01$, determined by Student's *t*-test).